Understanding sources and processes using chemistry of fine and coarse particles simultaneously collected from different windward locations in N-NW India

Sushil Kumar
Jawaharlal Nehru University
Sudesh Yadav (sudesh27@hotmail.com)
Jawaharlal Nehru University

Research Article

Keywords: Mineral dust, OC and EC, coefficient of divergence, Elements, Particle transport

DOI: https://doi.org/10.21203/rs.3.rs-258891/v1

Abstract

PM2.5and PM2.5-10 particles, simultaneously collected from Bikaner (BKR) and New Delhi (DEL) through Jhunjhunu (JHJ) located along S-SW wind pathduring summer in N-NW India were chemically characterized to understand their sourcesand related processes.Winds preferentially picked and trasnported PM2.5 compared to PM2.5-10 in windward direction. Ratios of mass concentrations and WSII in PM2.5 and PM2.5-10 were three or more at all sites. Thermal power plants, vehicles, and plastic burning were major contributors of SO42-, NO3- and Cl- ionsat DEL. Crustal materials, salt lakes/playas and contaminated aged particles were sources of WSIIs in PM2.5 over BKR and JHJ. In PM2.5, burning of wood and cow dung resulted in high OC/EC ratio (6.9) at BKR whereas EC emissions from vehicles lowered this ratio (3.5) at DEL. EC was dominated by char-EC compared to soot-EC. Major elements showed similar concentrations in both size particles but were depleted compared to Upper Continental Crustal (UCC) due to silica dilution effect. Ba and Sr, and Ba, Cr, Sr and Zn content showed site specific variations in PM2.5 and PM2.5-10, respectively. Trace elements in PM2.5 showed high enrichment compared to UCC at DEL due to re-suspension of roadside dust and vehicle related emissions.

Introduction

Arid regions over continents are potential sources of dust particles, which is transported to local, regional and continental scales by prevailing winds.[1,2,3,4,5] Wind-assisted transport of particles from desert regions influences air quality[6,5] human health[7,8] atmospheric chemistry[9,10], visibility[11] and nutrient dynamics[12]. Physical and chemical nature of atmospheric particles are variable with respect to their sources and size and are also influnced by metereological factors, secondary chemical processes and geographical location[13,14]. Fine particles ($PM_{2.5}$) are largely contributed by anthropogenic sources with high residence time and are inhaled while breathing and cause direct health effects compared to coarse particles[15,16].

New Delhi, the capital of India, is facing severe air quality problems during summer season due to wind-assisted transport of particles from the Thar Desert region in upwind direction[17,18,19]. Rapid urbanization, industrialization and transportation system further amplify the problems of air pollution in urban area of downwind (New Delhi) region[20,13,18]. Mixing of crustal particles with anthropogenic particles such as (sulphate, nitrate), organic carbon (OC), elemental carbon (EC) during long-range transport and deposition affects atmospheric chemistry[21,19]. Water-soluble Inorganic ions (WSIIs), OC, EC in particles are useful tool to understand anthropogenic sources and chemical interactions in ambient atmosphere whereas major (Al, Fe, Ca, Ti, Mn) and trace elements (Ba, Cd, Co, Pb, Cr, Cu, Zn) can be used as source signatures of crustal materials and anthropogenic sources such as fossil fuel combustion, abrasion of vehicle tire, and industrial emission [22,23, 24,19]. Studies conducted in past over N-NW India remained focused on PM_{10} and SPM in this region and have suggested significant influence of dust storm on ambient air quality[25,26,14]. In this work, simultaneous sampling of $PM_{2.5}$ and $PM_{2.5\text{-}10}$ was done at Bikaner located in active desert in upwind region, Jhunjhunu in paleo-desert region and New Delhi in downwind region in sub-humid climate. All sampling sites are located along S-SW wind corridor from west to east in north-northwest India. Samples were analyzed for WSII, OC, EC and for elements in the residue filter of water-soluble fraction to understand sources, processes and impact of S-SW winds on air quality and particles concentrations.

STUDY AREA

Study area for this work extended from great Indian Thar desert in the west to New Delhi for $PM_{2.5}$and $PM_{2.5\text{-}10}$sample collection during summer season in N-NW India (Fig.1). This region experiences transition in climate, meteorological conditions, geomorphic features, altitude from sea level, urbanization and industrialization on moving from west (Bikaner: 28.01ºN and 73ºE)) to east (New Delhi: 28.38ºN and 77.12ºE) through Jhunjhunu (28.06ºN and 75.25ºE)

covering a distance of 600 km. The Geat Indian Thar Desert in the west acts as potential source of particles and high intensity winds picks particles and transport them in windward direction. Particle carrying capacity of S-SW winds decreases along windward direction due to increase in elevation from sea level, Aravalli Mountains, more vegetation cover, and sub-humid climate (Fig.1). This study domain represents a unique geographical region, good natural laboratory for the studies on particle generation, transportation and depositional processes along dominant wind path during summer season and their environmental implications. More details about the study area can be accessed from our previous work [25,26,18]. Meteorological data for the study period were taken from Resources Laboratory: National Oceanic and Atmospheric Administration (ARL-NOAA) (http://www.arl.noaa.gov/). Cluster mean trajectories of air backward trajectories ending at the sampling sites BKR, JHJ and DEL during the sampling period May-2012 were calculated at two level 500m and 1000m above ground level (AGL) (Fig.2). Meteorological data (average wind speed, relative humidity, planetary boundary layer) over BKR,JHJ and DEL are provided in Supplementary Table S1 online.

Methodology

$PM_{2.5}$ and $PM_{2.5-10}$ particles were simultaneously collected for the period (May 2012) using mass flow controlled high volume air sampler (Tisch Environmental Inc) fitted with cascade impactors installed at rooftop of School of Environmental Sciences (SES) buildings in Jawaharlal Nehru University (JNU), New Delhi (DEL), and rooftop of house buildings located at Chakwas village near to Jhunjhunu (JHJ) city and at Udairamsar village near to Bikaner (BKR) city during summer season (Fig. 1). Sampling height at all sites vary between 8-10 m. Sampling sites were selected away from city to avoid any direct influence of pollution sources. $PM_{2.5}$ and $PM_{2.5-10}$ particles were collected on quartz fiber filters (QFFs) of 20×25 cm size and perforated QFFs of 13 ×18 cm size placed on impactor plates, respectively. Both types of QFFs were pre-combusted and pre-conditioned[18]. Each sample was collected for 24 h duration. A total of 32 samples of $PM_{2.5}$ and $PM_{2.5-10}$ each (11 at BKR, 9 at JHJ and 12 at DEL) were collected with a frequency of 2 or 3 samples per week during summer season. Some samples were rejected too in the field itself due to electricity problems, breakdown of instrument and damage of filters under strong windy conditions. Field blanks and laboratory blanks were also collected and handled in a manner similar to that of actual sample[18,19].

An aliquot of the sample filter was extracted in Milli Q water using ultra sonicator for major cations (Ca^{2+}, Mg^{2+}, Na^{+}, K^{+} and NH_4^{+}) and anions (F^{-}, Cl^{-}, NO_3^{-} and SO_4^{2-}) and analyzed using Metrohm Ion Chromatograph (IC) model 882 Compact IC plus1 pro1 equipped with conductivity channel installed at JNU, New Delhi. Field blank and laboratory blanks were also analyzed simultaneously with particle samples. More details on extraction and ion analysis can be accessed from our previous work [27,14,18]. Residue filter paper after extractions of WSII was digested following “B ” solution method [28]. Error and accuracy of the data was checked through analysis of digested standards, BHVO-2, GSP-2, SGR procured from United States Geological Survey. Elemental analysis was carried out using Inductively Coupled Plasma Optical Emission Spectrometer (ICP-OES). Multi-element and multi-ions standards, procured from E-Merck Germany, were used for calibration of ICP-OES and IC, respectively. All analysis was carried out in clean laboratories having 1000 airflow. Details of average recovery, repeatability, and correctness of WSII and elemental data are provided in the Supplementary Tables S2 and S3 online.

The OC and EC analysis was done using carbon analyzer (DRI model 2001, Atmoslytic Inc.) following IMPROVE_A thermal/optical reflectance (TOR) protocol [29]. In this protocol, the algorithm used for calculating OC and EC in particle samples on QFFs has been calibrated for 0.526 cm^2 area of QFFs. The OC and EC analysis was performed only in $PM_{2.5}$ as the perforated QFFs did not have the required punch area. The analyzer works on preferential oxidation of OC and EC at different temperatures which produced four operationally defined OC fractions (OC1, OC2, OC3 and OC4 at 140°C, 280°C, 480°C and 580°C, respectively in a helium [He] atmosphere) and OP (pyrolyzed carbon fraction), and three EC

fractions (EC1, EC2 and EC3 at 580°C, 740°C and 840°C in a 2% O_2 and 98% He atmosphere). The EC1 minus OP fraction represented low temperature EC, termed as char-EC, and EC2 and EC3 together represented high temperature EC, termed as soot-EC [30].

Results And Discussion

Mass Concentrations

Average $PM_{2.5}$ concentration increased along windward and was highest over DEL (568±527 μg m^{-3}) followed by JHJ (382±168 μg m^{-3}) and BKR (281±155 μg m^{-3}) (Table 1; Fig. 3). $PM_{2.5-10}$ concentration was also highest over DEL (162±162 μg m^{-3}) followed by BKR (95±93 μg m^{-3}) and JHJ (69± 33 μgm^{-3}). $PM_{2.5}$ concentration was observed as high as 1884 μg m^{-3}, 640 μg m^{-3} and 650 μg m^{-3} over DEL, BKR and JHJ due to dust storms observed on 18th, 15th, and 19th may 2012, respectively. Similar to $PM_{2.5}$, $PM_{2.5-10}$ concentration was also high over DEL followed by BKR and JHJ during these sampling dates. Sporadic dust storm events lead to high standard deviation in particle concentrations. On average basis, $PM_{2.5}$ contributed 75%-80% to PM_{10} (PM_{10} = $PM_{2.5}$ + $PM_{2.5-10}$) over three sampling sites (Table 1; Fig. 3), an observation similar to that reported over Raipur (India)[31]. Average $PM_{2.5}/PM_{2.5-10}$ mass concentration ratios were 2.97, 5.53 and 3.50 over BKR, JHJ and DEL sites, respectively (see Supplementary Table S4 online). Similar trends of high $PM_{2.5}$ compared to $PM_{2.5-10}$ have been reported previously[32, 33, 14] at different sites in India.

Particle generation (in source region; the Thar desert) and particle transport processes by high intensity S- SW winds were size selective in nature. Winds preferentially picked finer particles as evident from high $PM_{2.5}$ concentrations at all sites. An alternative explanation could also fit in here that coarse particles were also lifted but wind intensity could not sustain them in ambient atmosphere and they settled down under gravity effect and therefore, could not be captured in real time sampling. Relatively high $PM_{2.5-10}$ concentration (161 μgm^{-3}) at DEL could be due to local contributions from re-suspension activities [34]. Higher $PM_{2.5}/PM_{2.5-10}$ mass ratio at JHJ can be a location manifestation and attributed to relatively higher altitude compared to BKR and DEL on either side. Air quality remained worst hit during the sampling period as $PM_{2.5}$ and $PM_{2.5-10}$ load exceeded the national ambient air quality standard (NAAQS) of India for $PM_{2.5}$ (60μg m^{-3}). $PM_{2.5}$ load has intermittently exceeded the NAAQS by a factor of 10 and 31 at BKR and DEL, respectively. DEL could act as sink for particles transported from upwind region as the wind speed substantially decrease due to increased vegetation and elevation form sea level, Aravali mountains and the sub-humid climate. Transport of dust from desert region in west India and far west to New Delhi and Indo-Gangetic Plains (east to New Delhi) has also been observed through satellite data [35,16,36]. In addition to natural factors, New Delhi had own local sources such as vehicular and thermal power plant emissions.

Water-Soluble Inorganic Ions (WSIIs)

Average data on WSIIs in $PM_{2.5}$ and $PM_{2.5-10}$ collected from BKR, JHJ and DEL are provided in Table 1. Sea salt contributions to individual ions and ∑WSII in fine and coarse particles at all sites were very limited (Table 1) and therefore, only total concentrations of individual ions and ∑WSII in both size particles are discussed hereafter. Percentage contributions of ∑WSII to $PM_{2.5}$ and $PM_{2.5-10}$ concentrations showed an increase from BKR (4.9%) to DEL (13.2%) through JHJ (3.0%) in $PM_{2.5}$ and from 4.7% at BKR, 5.4% at JHJ to 12.7% at DEL in $PM_{2.5-10}$ (Table 1). At all sites, anions were dominated by SO_4^{2-}, NO_3^-, Cl^- and cations were dominated by Ca^{2+}, K^+, Na^+ and Mg^{2+} with limited amount of NH_4^+ in both size particles (Table 1; Fig. 4).Average ratio of ΣWSII in $PM_{2.5}$ and $PM_{2.5-10}$ ($PM_{2.5}/PM_{2.5-10}$) were around three or more at all sites but individual ion ratios were even higher and showed sampling site-specific variations (see Supplementary Table S4 and Fig. S1 online). Spatially, WSII in both size particles were present in nearly similar

concentrations in at BKR and JHJ sites, suggesting homogenizing effects of winds over upwind sites. The SO_4^{2-}, NO_3^- and Cl^- ions in $PM_{2.5}$ and $PM_{2.5-10}$ at DEL were substantially higher than those observed at BKR and JHJ sites. Other aspect was higher concentrations of Ca^{2+}, K^+, Na^+ and Mg^{2+} in both size fractions over DEL compared to other two sites except that Mg^{2+} was highest in $PM_{2.5}$ over JHJ and Na^+ was highest in $PM_{2.5-10}$ over BKR.

Average percentage contribution of each soluble ion to total $\sum$WSII in $PM_{2.5}$ and $PM_{2.5-10}$ are given in Supplementary Table S5 and Fig. S2 online. In $PM_{2.5,}$ sulfate ions contributed highest (36%-39%) to $\sum$WSII followed by Ca^{2+} (18% -20%), NO_3^- (14% -16%), Na^+ (11%) and K^+(5%) with 1% -2% contribution of NH_4^+ and Mg^{2+}at BKR and JHJ (see Supplementary Fig. S2 online). Over DEL too, sulfate contributed maximum (28%) to $\sum$WSII but followed by Cl~ NO_3^-(19-20%), Ca^{2+} (16%) and Na^+ (6%). Average percentage composition of $PM_{2.5-10}$ was different than that of $PM_{2.5}$ at all three sites. Sulfate ions contributed nearly equal to Na^+ (20% -21%) followed by NO_3^-~Cl^-~Ca^{2+} (17% -18%) over BKR whereas NO_3^- contributed maximum (30%) followed by Ca^{2+} (21%), Cl^-~SO_4^{2-} (15-17%) and Na^+ (10%) at JHJ site. Similar to JHJ site, $PM_{2.5-10}$ at DEL too had high NO_3^- (37%) but followed by Cl^- (32%), SO_4^{2-}~Ca^{2+} (11-12%).

These variations can be explained on the basis of wind speed, local sources specific to site(s), formation of secondary soluble ions (SSIs), adsorption of finer particles onto larger particles and inclusion of aged particles in $PM_{2.5}$ and $PM_{2.5-10}$. Increasing trend of SO_4^{2-}, NO_3^- and Cl^- from upwind to downwind region were related to high emissions of their precursor gases SO_2, NO_X, and Cl_2 from thermal power plant and vehicular emissions, and plastic burning, respectively at DEL site[14]. Beside this, SO_4^{2-} and NO_3^- are also contributed by crustal sources and remain present as $CaSO_4$, $Ca(NO_3)_2$ in mineral dust[37,38]. This was further supported by 36-39% contribution of SO_4^{2-} to $\sum$WSII over BKR and JHJ sites. Higher $PM_{2.5}/PM_{2.5-10}$ ratio of SO_4^{2-}, NO_3^-, NH_4^+ and F^- ions over BKR could be an indication of inclusion of aged particles in $PM_{2.5}$ as direct sources of these ions in upwind region are limited. The contributions of SO_4^{2-} and Ca^{2+} decreased towards DEL compared to BKR and JHJ at the cost of increase in nitrate at DEL. Vehicular emissions are potential source of NO_x which eventually oxidized to nitrate (NO_3^-, NH_4NO_3, HNO_3^-) and more so with mineral dust mediated oxidation during summer[39]. Influence of sea salt particles from far west and the presence of dried salt lakes and playas in upwind region could possibly explain high Cl^- and Na^+ at BKR and JHJ. New Delhi, being an inland site, was least affected by sea salt contributions. Similar high percentage contributions of Ca^{2+} and Na^+ in particle have been observed over Tunisia in North Africa and Jimei district of Xiamen city, mainly due to long-range transport of mineral dust and sea salts[40,39]. It has been observed that Cl^- over DEL comes from fossil fuel burning (coal combustion), brick kilns and biomass burning. Chlorine particles react with SO_2 and NO_X to form hydrochloric acid. Burning of crop residue and biomass, and emissions from vegetation are important source of potassium ions over DEL site[41,42,43].

Molar Ratios of Ions and Neutralization Factors (NF)

To understand particle acidity and neutralization processes, neutralization factors (NF) for cation(s) were computed using molar concentrations (meq L^{-1}) following the equation $NF_X = [X/SO_4^{2-} + NO_3^-]$ where X is the cation for which NF was computed (see Supplementary Table S6 online).Alkaline nature of water-soluble fractions of both size particles of all sites compared to natural rainwater pH indicated sufficient neutralization of acid forming ions by cations. Ca^{2+} ions followed by Mg^{2+} were dominant neutralizing cations. Low NF values for NH_4^+ could be due to photo-dissociation of ammonium nitrate or even limited conversion of NH_3 to NH_4^+ due to high temperature conditions during summer. In and around DEL site, NH_4^+ has been reported as potential neutralizing cation in particle, fog, dew and rainwater in winter season when stability and solubility of ammonium compounds is favored[44,45]. The Ca^{2+} ions in particles could have

come from primary and secondary carbonates as well as from reactions between carbonates of calcium and acids such as H_2SO_4, HNO_3 and HCl[46].

Further, inter-ionic correlations were drawn to observe ionic associations in particles (Table 2). Poor correlations among ions in $PM_{2.5}$ (at 0.01 confidence level) were observed at all sites except that Ca^{2+} and Mg^{2+} were closely associated with SO_4^{2-} (r= 0.88 or more) at BKR and K^+ was related to NO_3^- at JHJ site. Compared to $PM_{2.5}$, good correlations at 0.01 confidence level among soluble ions were observed in $PM_{2.5-10}$. SO_4^{2-} and NO_3^- showed a good correlation suggesting their common sources which could be crustal at BKR and anthropogenic at DEL. Correlation of Na^+ with Cl^-, NO_3^- and SO_4^{2-} at BKR suggested their common sources as salt lakes and playas. Mg^{2+} and NO_3^- correlation are too indicative of their common marine sources which in present case could be salt lakes[21, 47]. At DEL site, Na^+ and K^+ showed good correlation with SO_4^{2-} and NO_3^- (r = 0.84-0.94 at 0.01 level) in coarse particles. Na^+ did show good correlation with NH_4^+ (r= 0.81). Particles during the aging processes get coated by other ions or adsorption of gases or moisture and represent unusual chemical associations in particle[21,48].

OC and EC in $PM_{2.5}$

Average OC, EC and TC (TC = OC+EC) concentrations in $PM_{2.5}$ with other related parameters are provided in Table 3 and are plotted in Fig. 5. TC was highest over DEL (avg: 36.5 μgm^{-3}) followed by BKR (avg: 12.9μgm^{-3}) and JHJ (avg: 9.0 μgm^{-3}) (Table 3). TC contribution to $PM_{2.5}$ was highest at DEL (9.2%) followed by BKR (4.8%) and JHJ (2.4%). Total carbon was dominated by OC compared to EC. Percentage OC contribution to TC in $PM_{2.5}$ decreased towards downwind sites as: BKR (87.3%) >JHJ (84.9%) > DEL (77.9%), while EC contributions increased towards downwind site as: BKR (12.7%) < JHJ (15.1%) < DEL (22.1 %). The OC/EC ratio showed wide variations both within and among the sampling sites. Average OC/EC ratio was 3.5 at DEL, 5.4 at JHJ and 6.9 at BKR (Table 3).Similar OC/EC ratios have also been reported at other urban sites in India; Patiala (8.7) [41], Agra (6.7) [49], Udaipur (6.4) and Jabalpur (4.8)[50]. Burning of wood and cow dung at domestic levels might have resulted in high OC/EC ratio (6.9) at BKR whereas more sources of EC such as vehicular emissions and other combustion processes have resulted in lower OC/EC ratios (3.5) at DEL [30]. The OC/EC ratios are influenced by their direct sources, secondary organic aerosol formation, and removal rate of carbonaceous aerosol[51,30].

POC and SOC calculations

Direct measurements of POC and SOC are difficult using OC-EC analyzer. Therefore, SOC in $PM_{2.5}$ was calculated by subtracting POC from measured OC and POC was calculated following the EC tracer method using $(OC/EC)_{min}$ ratio[52,53]. The contributions of POC and SOC to OC in $PM_{2.5}$ are shown graphically in Fig. 5. SOC concentrations and its contribution in OC showed a decline towards upwind site as: DEL (20.8 $\mu g\ m^{-3}$; 69.4%) → BKR (6.9 $\mu g\ m^{-3}$; 42.4 %) → JHJ (5.4 $\mu g\ m^{-3}$; 35.0 %). High SOC contributions to OC in DEL (69.4%) can be attributed to photo-oxidation of volatile organic compounds (VOC)[54,14]. Presence of VOCs, photochemical activity (solar radiation) and oxidizing agents such as O_3, OH radical, NO_X also help in formation of secondary organic particle (SOA)[55,56]. However, the observed SOC over BKR and JHJ could be a result of mineral particle mediated photo-oxidation of POC [14,18].

Total Carbonaceous Matter (TCM)

TCM represents total sum of organic matter (OM) and elemental matter (EM). OC was multiplied with a factor of 1.6 for urban areas (DEL) and with 2.1 for rural areas (BKR and JHJ) to get OM while EM was calculated from EC using a factor of 1.1 for urban as well as rural areas[52]. Highest contribution of TCM was observed over DEL (13.3%) followed by BKR

(9.4%) and JHJ (4.6%), respectively. The TCM was dominated by organic matter compared to elemental matter over all sites.

Carbon Fractions and Source Identification

Total eight carbon fractions (OC1, OC2, OC3, OC4, OP, EC1, EC2 and EC3) were analyzed and each fraction can be used to distinguish source(s)[57,58]. Concentration of each fraction and their percentage contribution in TC showed different trends over each sampling site (see Supplementary Table S7 and Fig. S3 online) and the percentage contribution of each fraction to TC is shown graphically in the Supplementary Fig. 3 online. The OC2, OC3 and OC4 contributed above 10% to TC and their concentrations increased from BKR to DEL while their percentage contribution to TC deceased from BKR to DEL. This was so because of increased EC compared to OC at DEL. OC1 was present in lowest amounts at all sites. Both concentrations and contributions of OP to TC increased along windward direction and were highest over DEL, possibly due to high contributions of water-soluble polar components in $PM_{2.5}$ over DEL[58,59,14]. The EC1 (char- EC) was more than soot-EC and was highest over DEL followed by BKR and JHJ due to smoldering combustion, biomass burning, coal combustion, vehicular emission[60,30].

Principal component analysis (PCA) has been applied for source identification of eight carbon fractions in $PM_{2.5}$[51]. Principle components having eigen value of greater than one were only considered(Table 4). Only one component could be extracted for BKR site with loading of OC2, OC3, OC4, EC1, EC2 and EC3, which explained 76.7% of the data variance. As we move in windward direction, two components over JHJ and three components over DEL were noticed. PC1 explained 74.9% of total variance with high loading of OC2, OC3, OC4, EC2 and EC3 while PC2 explained 23.4% of total variance with high loading of EC1 and OP. This suggested low temperature burning contributions over JHJ along with other sources. Three components PC1, PC2 and PC3 were identified over DEL which could explain 93.2% of variance. PC1 explained 36.4% of total variance with highest loading of OC2, OC3 and OC4 indicating emission from biomass burning, motor vehicle exhaust, road dust while PC2 explained 33.1% variance with highest loading of EC2 and OP and was linked to vehicle exhaust or condensation of volatile compounds. PC3 explained 23.8% variance with highest loading of EC1 and EC3 and was linked to biomass and coal combustion sources. Homogenization of direct carbon sources and surface materials by high intensity winds could be possible reason for one component at BKR. The component segregation over JHJ and DEL could be an outcome of poor homogenization effects due to lowering of wind speed in windward direction and the additional burden of carbon sources over DEL, a mega city.

Elemental Distribution

The statistical data on concentrations of major elements (Al, Ca, Fe, Mn and Ti; in μg m^{-3} units) and trace elements (Ba, Cd, Co, Cr, Cu, Pb, Sr and Zn; in ng m^{-3} units) in the residue of water-soluble fractions of $PM_{2.5}$ and $PM_{2.5-10}$ over BKR, JHJ and DEL are provided in Supplementary Table S8 online and graphically shown in (Fig. 6). Among two sizes, major elements were enriched in $PM_{2.5}$ compared to $PM_{2.5-10}$ at all sites, a observation similar to $PM_{2.5}$ and $PM_{2.5-10}$ concentrations. Al, Ti and Mn showed very similar concentrations at all sites in $PM_{2.5}$ and $PM_{2.5-10}$ except that Al showed site specific variations in $PM_{2.5-10}$ only (Fig. 6). Fe and Ca showed variations in both fine and coarse particles with respect to sampling sites and were highest over DEL in $PM_{2.5}$. In $PM_{2.5-10}$, Al, Ca and Fe were highest over BKR and lowest over JHJ in both size of particles (Fig. 6). Higher concentrations in $PM_{2.5-10}$ at BKR were due to low silica dilution effect on concentrations of major elements. Quartz grains hosting silica being larger in size and heavier in mass were subjected to winnowing away effect and therefore, were not picked by winds from the source region at BKR and JHJ sites[25]. Re-suspension of sediments lying on famous Delhi quartzite could have added silica rich particles to $PM_{2.5-10}$ and caused silica dilution effect on major elements at DEL site[61, 25].

Similar to major elements, trace elements were also higher in $PM_{2.5}$ compared to $PM_{2.5-10}$ overall sampling sites (Fig. 6). Among the sites, all trace elements were present in highest concentrations over in DEL in both size particles. Cd and Co were present in lowest amounts in both size fractions and showed similar concentrations at all sites. Concentrations of Cr, Cu and Pb were very similar over BKR and JHJ sites and were lower than that observed at DEL in both size particles. Ba and Sr in $PM_{2.5}$ and Ba, Cr, Sr and Zn in $PM_{2.5-10}$ showed sampling site specific variations, although their concentrations were high in DEL samples (Fig. 6). Cr finds mixed origin in particle in this region[25] and could have been added by minerals in upwind region and by re-suspension of anthropogenically contaminated roadside dust at DEL. Ba and Zn are contributed by vehicular emissions, oil burning and wear and tear of tyres and vehicular parts [62].

To better understand spatial variations in elemental composition of particles along dominant wind path, major and trace element concentrations in $PM_{2.5}$ and $PM_{2.5-10}$ of different sites are plotted in equiline plot (Fig. 7). Major element over BKR and JHJ in $PM_{2.5}$ are plotting on equiline while in $PM_{2.5-10}$ particles element enriched towards BKR due poor silica dilution effect over BKR as discussed before. On moving towards downwind (DEL), Ca and Fe get enrich on account of re-suspension of road dust and industrial emission (Fig. 7)[23]. Trace element distribution between BKR and JHJ are almost similar in $PM_{2.5}$ and $PM_{2.5-10}$ while with DEL enrichment in Cu, Cr, Pb Ba observe in both size particles suggesting influence of vehicular, industrial emission and re-suspension of road dust[23, 24]. Uniform composition over BKR and JHJ indicate common crustal sources and homogenization effect of winds on particle composition. This was also revealed through calculations of Coefficient of Divergence (CD), a dimensionless qualitative measure of homogeneity/heterogeneity in particle chemistry of different sampling sites (see Supplementary Table S9 online)[63]. The calculated CD values considering a) WSII only, b) WSII, OC and EC, c) WSII, OC, EC and elements, and d) WSII, OC, EC and elements for different sets of two sites in the region are provided in Supplementary Table S9 online**.** Two upwind sampling sites BKR and JHJ showed CD values for $PM_{2.5}$ close to 0.2 indicating spatial homogeneity for WSII and OC and elemental distribution in $PM_{2.5}$. The CD values for $PM_{2.5-10}$ were in the range of 0.34 and 0.38 indicating less mixing effect and homogeneity compared to $PM_{2.5}$ among BKR and JHJ sampling sites. The CD values for both size particles among JHJ and DEL were nearly double for $PM_{2.5}$ and 1.5 times for $PM_{2.5-10}$ compared to those observed for BKR and JHJ. This suggested that homogenization effects decreased over JHJ and DEL sampling sites. The two end members, BKR and DEL showed spatial heterogeneity with nearly double the CD values in $PM_{2.5}$ compared to that observed for BKR and JHJ and slightly higher in $PM_{2.5-10}$. The reason could be both lowering of wind speed and additional local anthropogenic sources of particles at DEL, which were very limited over JHJ and BKR sites.

In order to differentiate between natural (crustal) and cultural (anthropogenic) sources, Al normalized enrichment ratios (ER) of elements in $PM_{2.5}$ and $PM_{2.5-10}$ with respect to Upper Continental Crustal (UCC) were calculated (see Supplementary Table S10 online). Aluminum, being immobile element in geochemical process, is considered as good indicator of crustal sources[25,26,32]. Usually, a numerical value of two or more of ER is an indicative of anthropogenic contributions. All major elements except Ca showed less than one value of ER in both types of particle over all sampling sites in the Supplementary Table S10. This could be due to silica dilution effect on major elements while high ER of Ca could be on account of additional contributions from carbonates of calcium abundantly available in this region. Among trace elements, Ba, Cr, Cu, Pb and Zn showed higher ER at all sites. Like the concentrations, ERs were higher in $PM_{2.5}$ compared to that in $PM_{2.5-10}$ at all sites. The ERs of Cr, Cu and Pb were higher at BKR and DEL compared to JHJ. To note, the ERs of Cr, Cu were nearly double in $PM_{2.5}$ over DEL compared to that over BKR whereas the ER of Pb and Zn was nearly 17 times and 4 times compared to those observed at BKR site. In $PM_{2.5-10}$, ER of Cr, Cu, Pb, Ba and Zn were higher (~2 times or more) in DEL compared to that observed at BKR site suggesting anthropogenic contributions.

Conclusions

$PM_{2.5}$ and $PM_{2.5-10}$ mass concentrations and spatial variations suggested that 1) prevailing S-SW winds are responsible for high particle concentrations and air quality remained worst hit, particularly for $PM_{2.5}$ and 2) wind action in the Thar desert (source) region contribute more $PM_{2.5}$ compared to $PM_{2.5-10}$ particles. Particles in upwind regions were largely crustally derived particles and had low WSIIs (nearly 5%) compared to nearly 13% over DEL due to more anthropogenic sources. Vehicular emissions, thermal power plants, plastic burning and brick kiln industry are dominantly responsible source for high SSIs over DEL. Burning of wood and cow dung at domestic levels were major reasons for high OC/EC ratio at BKR whereas EC contributed by vehicular emissions and other combustion processes have resulted in lower of OC/EC ratio at DEL. Mineral dust mediated photo-oxidation of POC emitted by biomass burning could be possible source of SOC at BKR and JHJ whereas high SOC over DEL could be linked to photochemical reactions among NO_x and VOC, emitted from direct sources. Silica dilution effects resulted in lowering of major element concentrations compared to UCC. Trace elements found their crustal origin in upwind region while re-suspension of surface/road side dust and direct emission from vehicle and wear and tear of vehicle parts caused high ER of trace elements over DEL. Variations in water-soluble inorganic ions and elements were specific to particle size, and sampling site and was caused by multiple sources and subsequent process in ambient atmosphere. Upwind sites (BKR and JHJ) experience homogenization due to mixing by winds, whereas heterogeneity was noticed between DEL-JHJ, in downwind region and among DEL-BKR sites.

Declarations

Acknowledgment: Extra mural research project grants (24(0316)/11-EMR-II received by SY from Council of Scientific and Industrial Research (CSIR), New Delhi for carrying this work are duly acknowledged. SK is also thankful to UGC-BSR for research fellowship during this work. Grants received from DST–PURSE and utilized to carry our part of the work are duly acknowledged.

References

1. Jeong, G.Y., Park, M.Y., Kandler, K., Nousiainen, T., Kemppinen, O. Mineralogical properties and internal structures of individual fine particles of Saharan dust. Atmos. Chem. Phys. **16**, 12397-12410(2016).
2. Bozlaker, A., Prospero, J.M., Price, J., Chellam, S. Linking Barbados mineral dust aerosols to North African sources using elemental composition and radiogenic Sr, Nd, and Pb isotope signatures. J. Geophys.Res. Atmos.**123**, 1384-1400(2018).
3. Kumar, A., Abouchami, W., Galer, S.J.G., Singh, S.P., Fomba, K.W., Prospero, J.M., Andreae, M.O. Seasonal radiogenic isotopic variability of the African dust outflow to the tropical Atlantic Ocean and across to the Caribbean. Earth Planet. Sci. Lett. **487**, 94-105(2018).
4. Barkley, A.E., Prospero, J.M., Mahowald, N., Hamilton, D.S., Popendorf, K.J., Oehlert, A.M., Pourmand, A., Gatineau, A., Panechou-Pulcherie, K., Blackwelder, P. and Gaston, C.J. African biomass burning is a substantial source of phosphorus deposition to the Amazon, Tropical Atlantic Ocean, and Southern Ocean. Proc. Natl. Acad. Sci. **116**, 16216-16221(2019).
5. Querol, X., Pérez, N., Reche, C., Ealo, M., Ripoll, A., Tur, J., Pandolfi, M., Pey, J., Salvador, P., Moreno, T., Alastuey, A.African dust and air quality over Spain: Is it only dust that matters?. Sci. Total Environ. **686**, 737-752(2019).
6. Tsai, J.H., Huang, K.L., Lin, N.H., Chen, S.J., Lin, T.C., Chen, S.C., Lin, C.C., Hsu, S.C., Lin, W.Y.Influence of an Asian dust storm and Southeast Asian biomass burning on the characteristics of seashore atmospheric aerosols in southern Taiwan. Aerosol Air Qual. Res. **12**, 1105-1115(2012).
7. Pope, III C.A., Dockery, D.W.Health effects of fine particulate air pollution: lines that connect. J. Air Waste Manag. Assoc. **56**, 709-742 (2006).

8. Deng, Q., Deng, L., Miao, Y., Guo, X., Li, Y. Particle deposition in the human lung: Health implications of particulate matter from different sources. Environ. Res.**169**, 237-245(2019).
9. Pavuluri, C.M., Kawamura, K., Aggarwal, S.G., Swaminathan, T. Characteristics, seasonality and sources of carbonaceous and ionic components in the tropical aerosols from Indian region. Chem. Phys.**11**, 8215-8230(2011).
10. Wang, J., Hu, Z., Chen, Y., Chen, Z., Xu, S.Contamination characteristics and possible sources of PM_{10} and PM_5 in different functional areas of Shanghai, China. Atmos. Environ.**68**, 221-229(2013).
11. Singh, A., Dey, S.Influence of aerosol composition on visibility in megacity Delhi. Environ.**62**, 367-373(2012).
12. Jickells, T.D., An, Z.S., Andersen, K.K., Baker, A.R., Bergametti, G., Brooks, N., Cao, J.J., Boyd, P.W., Duce, R.A., Hunter, K.A., Kawahata, H. Global iron connections between desert dust, ocean biogeochemistry, and climate. **308**, 67-71(2005).
13. Behera, S.N., Sharma, M. Spatial and seasonal variations of atmospheric particulate carbon fractions and identification of secondary sources at urban sites in North India. Environ. Sci. Pollut. Res. **22**, 13464-13476 (2015).
14. Kumar, P., Yadav, S.Seasonal variations in water soluble inorganic ions, OC and EC in PM_{10} and $PM_{>10}$ aerosols over Delhi: Influence of sources and meteorological factors. Aerosol Air Qual. Res. **16**, 1165-1178(2016).
15. David, L.M., Ravishankara, A.R., Kodros, J.K., Pierce, J.R., Venkataraman, C., Sadavarte, P.Premature mortality due to PM_5 over India: Effect of atmospheric transport and anthropogenic emissions. Geohealth. **3**, 2-10(2019).
16. Sarkar, S., Chauhan, A., Kumar, R., Singh, R.P.Impact of Deadly Dust storms (May 2018) on Air Quality, Meteorological and Atmospheric Parameters over the Northern Parts of India. Geoheal. **3**, 67-80(2019).
17. Guttikunda, S.K., Goel, R., Pant, P.Nature of air pollution, emission sources, and management in the Indian cities. Environ.**95**, 501-510(2014).
18. Kumar, P., Kumar, S., Yadav, S. Seasonal variations in size distribution, water –soluble ions, and carbon content of size- segregated aerosols over New Delhi. Environ. Sci. Pollut. Res. **25**, 6061-6078(2018).
19. Kumar, S. and Yadav S.Chemistry of size-segregated particles: study of sources and processes in N-NW India. Atmos. Poll. Res. **11**, 370-382(2020).
20. Liu, X.G., Li, J., Qu, Y., Han, T., Hou, L., Gu, J., Chen, C., Yang, Y., Liu, X., Yang, T., Zhang, Y.Formation and evolution mechanism of regional haze: a case study in the megacity Beijing, China. Chem. Phys.**13**, 4501-4514(2013).
21. Srinivas, B., Sarin, M.M. PM_5, EC and OC in atmospheric outflow from the Indo-Gangetic Plain: Temporal variability and aerosol organic carbon-to-organic mass conversion factor. Sci. Total Environ. **487**, 196-205(2014).
22. Zhang, Y., Mahowald, N., Scanza, R.A., Journet, E., Desboeufs, K., Albani, S., Kok, J.F., Zhuang, G., Chen, Y., Cohen, D.D., Paytan, A. Modeling the global emission, transport and deposition of trace elements associated with mineral dust. Biogeosci. **12**,5771-5792(2015).
23. Soleimani, M., Amini, N., Sadeghian, B., Wang, D., Fang, L.Heavy metals and their source identification in particulate matter (PM_5) in Isfahan City, Iran. J. Environ. Sci. **72**,166-175(2018).
24. Wu, X., Chen, B., Wen, T., Habib, A., Shi, G.Concentrations and chemical compositions of PM_{10} during hazy and non-hazy days in Beijing. J. Environ. Sci. **87**, 1-9(2019).
25. Yadav, S., Rajamani, V.Geochemistry of aerosols of north western part of India adjoining the Thar desert1. Cosmochim. Ac.**68**, 1975-1988(2004).
26. Yadav, S., Rajamani, V.Air quality and trace metal chemistry of different size fractions of aerosols in N–NW India—implications for source diversity. Environ.**40**, 698-712(2006).
27. Kumar, P., Yadav, S., Kumar, A.Sources and processes governing rainwater chemistry in New Delhi, India. Nat. Haz.. **74**, 2147-2162(2014).

28. Pruseth, K. L., Yadav, S., Mehta, P., Pandey, D., Tripathi, J. K.Problems in microwave digestion of high-Si and high-Al rocks. Sci. **89**, 1668-1671(2005).
29. Chow, J.C., Watson, J.G., Chen, L.W.A., Chang, M.O., Robinson, N.F., Trimble, D., Kohl, S.The IMPROVE_A temperature protocol for thermal/optical carbon analysis: maintaining consistency with a long-term database. J. Air Waste Manage. **57**, 1014-1023(2007).
30. Han, Y.M., Cao, J.J., Lee, S.C., Ho, K.F., An, Z.S. Different characteristics of char and soot in the atmosphere and their ratio as an indicator for source identification in Xi'an, China. Chem. Phys.**9**, 13271-13298(2009).
31. Deshmukh, D.K., Deb, M.K., Mkoma, S.L.Size distribution and seasonal variation of size-segregated particulate matter in the ambient air of Raipur city, India. Air Qual. Atmos. Health. **6**, 259-276(2013).
32. Rengarajan, R., Sudheer, A. K., Sarin, M.M.Wintertime PM_5 and PM_{10} carbonaceous and inorganic constituents from urban site in western India. Environ. Res. **102**, 420-431(2011).
33. Ram, K., Sarin, M.M.Atmospheric carbonaceous aerosols from Indo-Gangetic Plain and Central Himalaya: Impact of anthropogenic sources. J Environ. Manag.**148**, 153-163(2015).
34. Tandon, A., Yadav, S., Attri, A.K.City-wide sweeping a source for respirable particulate matter in the atmosphere. Environ.**42**,1064-1069(2008).
35. Moorthy, K.K., Satheesh, S.K., Kotamarthi, V.R. Evolution of aerosol research in India and the RAWEX–GVAX: an overview. Sci. 111, 53-75(2016).
36. Mangla, R., Indu, J., Chakra, S.S. Inter-comparison of multi-satellites and Aeronet AOD over Indian Region. Res.240, 104950 (2020).
37. Radhi, M., Box, M.A., Box, G.P., Mitchell, R.M., Cohen, D.D., Stelcer, E., Keywood, M.D.Size-resolved mass and chemical properties of dust aerosols from Australia's Lake Eyre Basin. Environ.**44**, 3519-3528(2010).
38. Tobo, Y., Zhang, D., Matsuki, A., Iwasaka, Y.Asian dust particles converted into aqueous droplets under remote marine atmospheric conditions. Natl. Acad. Sci.**107**, 17905-17910(2010).
39. Zhao, J., Zhang, F., Xu, Y., Chen, J. Characterization of water-soluble inorganic ions in size-segregated aerosols in coastal city, Xiamen. Res.**99**, 546-562(2011).
40. Kchih, H., Perrino, C., Cherif, S. Investigation of desert dust contribution to source apportionment of PM_{10} and PM_5 from a southern Mediterranean coast. Aerosol Air Qual. Res. **15**, 454-464(2015).
41. Rastogi, N., Singh, A., Singh, D., Sarin, M.M.Chemical characteristics of PM_5 at a source region of biomass burning emissions: Evidence for secondary aerosol formation. Environ. Pollut. **184**, 563-569(2014).
42. Andreae, M.O., Merlet, P. Emission of trace gases and aerosols from biomass burning. Global Biogeochem. Cycl. **15**, 955-966 (2001).
43. Singh, R., Kulshrestha, M.J., Kumar, B., Chandra, S.Impact of anthropogenic emissions and open biomass burning on carbonaceous aerosols in urban and rural environments of Indo-Gangetic Plain. Air Qual. Atmos. Healt. **9**, 809-822(2016).
44. Yadav, S., Kumar, P. Pollutant scavenging in dew water collected from an urban environment and related implications. Air Qual. Atmos. Health. **7**, 559-566(2014).
45. Nath, S. and Yadav, S.A Comparative Study on Fog and Dew Water Chemistry at New Delhi, India.Aerosol Air Qual. Res.**18**, 26–36(2018).
46. Wei, N., Xu, Z., Liu, J., Wang, G., Liu, W., Zhuoga, D., Xiao, D., Yao, J. Characteristics of size distributions and sources of water-soluble ions in Lhasa during monsoon and non-monsoon seasons. J. Environ. Sci. **82**, 155-168(2019).
47. Lu, Z., Liu, X., Zhang, Z., Zhao, C., Meyer, K., Rajapakshe, C., Wu, C., Yang, Z.,Penner, J.E.Biomass smoke from southern Africa can significantly enhance the brightness of stratocumulus over the southeastern Atlantic Ocean.

Natl. Acad. Sci. **115**, 2924-2929(2018).

48. Sudheer, A.K., Aslam, M.Y., Upadhyay, M., Rengarajan, R., Bhushan, R., Rathore, J.S., Singh, S.K., Kumar, S.Carbonaceous aerosol over semi-arid region of western India: Heterogeneity in sources and characteristics. Atmos. Res. **178**, 268-278(2016).
49. Pachauri, T., Satsangi, A., Singla, V., Lakhani, A., Kumari, K.M. Characteristics and sources of carbonaceous aerosols in PM_5 during wintertime in Agra, India. Aerosol Air Qual. Res. **13**, 977-991(2013).
50. Panicker, A.S., Ali, K., Beig, G., Yadav, S.Characterization of particulate matter and carbonaceous aerosol over two urban environments in Northern India. Aerosol Air Qual. Res. **15**, 2584 -2595(2015).
51. Cao, J.J., Wu, F., Chow, J.C., Lee, S.C., Li, Y., Chen, S.W., An, Z.S., Fung, K.K., Watson, J.G., Zhu, C.S., Liu, S.X. Characterization and source apportionment of atmospheric organic and elemental carbon during fall and winter of 2003 in Xi'an, China. Chem. Phys.**5**, 3127-3137(2005).
52. Yttri, K.E., Dye, C., Kiss, G. Ambient aerosol concentrations of sugars and sugar-alcohols at four different sites in Norway. Chem. Phys.**7**, 4267-4279(2007).
53. Hu, W.W., Hu, M., Deng, Z.Q., Xiao, R., Kondo, Y., Takegawa, N., Zhao, Y.J., Guo, S., Zhang, Y.H. The characteristics and origins of carbonaceous aerosol at a rural site of PRD in summer of 2006. Chem. Phys.**12**, 1811-1822(2012).
54. Castro, L.M., Pio, C.A., Harrison, R.M., Smith, D.J.T. Carbonaceous aerosol in urban and rural European atmospheres: estimation of secondary organic carbon concentrations. Environ. **33**, 2771-2781(1999).
55. Lim, Y.B., Tan, Y., Perri, M.J., Seitzinger, S.P., Turpin, B. J.Aqueous chemistry and its role in secondary organic aerosol (SOA) formation. Chem. Phys. **10**, 10521-10539(2010).
56. Rastogi, N., Patel, A., Singh, A., Singh, D.Diurnal variability in secondary organic aerosol formation over the Indo-Gangetic Plain during winter using online measurement of water-soluble organic carbon. Aerosol Air Qual. Res. **15**, 2225-2231(2015).
57. Chow, J.C., Watson, J.G., Kuhns, H., Etyemezian, V., Lowenthal, D.H., Crow, D., Kohl, S.D.,Engelbrecht, J.P., Green, M.C.Source profiles for industrial, mobile, and area sources in the Big Bend Regional Aerosol Visibility and Observational study. Chemosph. **54**, 185-208(2004).
58. Gu, J., Bai, Z., Liu, A., Wu, L., Xie, Y., Li, W., Dong, H., Zhang, X. Characterization of atmospheric organic carbon and element carbon of PM_5 and PM_{10} at Tianjin, China. Aerosol Air Qual. Res. **10**, 167-176(2010).
59. Zhang, X., Liu, Z., Hecobian, A., Zheng, M., Frank, N.H., Edgerton, E.S., Weber, R.J. Spatial and seasonal variations of fine particle water-soluble organic carbon (WSOC) over the southeastern United States: implications for secondary organic aerosol formation. Chem. Phys. **12**,6593-6607(2012).
60. Han, L., Zhuang, G., Cheng, S., Li, J.The mineral aerosol and its impact on urban pollution aerosols over Beijing, China. Environ. **41**, 7533-7546(2007).
61. Tripathi, J.K., Rajamani, V.Geochemistry of the loessic sediments on Delhi ridge, eastern Thar desert, Rajasthan: implications for exogenic processes.Chem. Geol.**155**, 265-278(1999).
62. Morawska, L., Zhang, J.J.Combustion sources of particles. 1. Health relevance and source signatures. **49**, 1045-1058(2002).
63. Shen, Z., Cao, J., Liu, S., Zhu, C., Wang, X., Zhang, T., Xu, H., Hu, T. Chemical composition of PM_{10} and PM_5 collected at ground level and 100 meters during a strong winter-time pollution episode in Xi'an, China. J. Air Waste Manage. **61**, 1150-1159(2011).

Tables

Table 1. Statistical details of data on mass loading, water-soluble inorganic ions and non-sea salt (nss) fractions (in μgm^{-3} units) and their percentage contributions to $PM_{2.5}$ and $PM_{2.5-10}$ collected during summer season over Bikaner (BKR), Jhunjhunu (JHJ) and New Delhi (DEL) in North West India.

	BKR		JHJ		DEL	
	$PM_{2.5}$	$PM_{2.5-10}$	$PM_{2.5}$	$PM_{2.5-10}$	$PM_{2.5}$	$PM_{2.5-10}$
Mass	281.5±155.4(143.4-639.7)^	94.6±93.3(41.6-348.5)	382.4±168.3(184.3-650.4)	69.1±33.2(40.2-117.8)	568±526.9(232.2-1884.5)	161.9±161.9(86.9-452.4)
%Mass*	75.7±10.2(62.2-81.9)	24.3±10.2 (18.1-37.8)	84.6±3.1(80.9-87.7)	15.4±3.1(12.2-19.1)	75.3±8.1(60.4-88.9)	24.7±8.8(11.1-39.6)
F^-total$^-$	0.05±0.04(0.03-0.2)	0.01±0.01(0.01-0.04)	0.05±0.02(0.03-0.09)	0.01±0.01(0.01-0.02)	0.2±0.1(0.1-0.6)	0.1±0.1(0.04-0.2)
Cl^-total	1.2±0.6(0.4-2.1)	0.7±0.4(0.2-1.5)	0.8±0.4(0.3-1.5)	0.6±0.5(0.2-1.5)	8.7±7.0(2.8-20.0)	4.8±2.5(1.1-8.3)
NO_3^-total$^-$	1.7±0.8(1.2-2.8)	0.7±0.4(0.1-1.1)	1.7±0.8(1.0-2.8)	1.0±0.2(0.7-1.2)	12.5±21.2(2.1-68.3)	6.5±6.2(0.8-21.5)
SO_4^{2-}total	4.3±1.5(0.8-6.0)	0.8±0.4(0.2-1.7)	4.1±1.4(2.8-6.3)	0.5±0.2(0.3-0.8)	10.4±3.0(7.7-17.5)	1.4±0.6(0.8-2.6)
nss-SO_4^{2-}	4.1±1.5(0.6-5.5)	0.6±0.3(0.1-1.2)	3.8±1.3(2.6-6.0)	0.4±0.2(0.3-0.6)	9.8±2.6(7.2-16.0)	1.2±0.6(0.7-2.4)
NH_4^+total	0.1±0.1(0.1-0.3)	0.01±0.02(0.01-0.05)	0.1±0.1(0.1-0.3)	0.05±0.02(0.03-0.08)	0.3±0.3(0.05-0.9)	0.01±0.02(0.01-0.04)
Na^+total	1.2±0.5(0.6-2.2)	0.8±0.4(0.4-1.7)	1.1±0.4(0.6-1.5)	0.4±0.2(0.2-0.7)	2.3±1.4(1.5-6.0)	0.6±0.3(0.4-1.2)
K^+total	0.7±0.4(0.2-1.5)	0.2±0.2(0.1-0.6)	0.6±0.3(0.3-1.1)	0.1±0.04(0.1-0.2)	3.0±0.9(1.1-4.0)	0.3±0.2(0.1-0.6)
$\$_{nss-K^+}$	0.6±0.4(0.2-1.4)	0.2±0.2(0.1-0.6)	0.5±0.3(0.3-1.1)	0.1±0.03(0.08-0.16)	2.9±0.9(1.0-3.8)	0.3±0.2(0.1-0.6)
Ca^{2+}total	2.3±1.2(0.8-5.5)	0.7±0.4(0.3-1.6)	1.8±0.2(1.5-2.0)	0.7±0.1(0.6-0.8)	5.9±3.1(3.6-13.3)	1.6±0.6(0.9-2.5)
nss-Ca^{2+}	2.2±1.2(0.8-5.4)	0.6±0.4(0.2-1.6)	1.8±0.2(1.5-2.0)	0.7±0.1(0.6-0.8)	5.8±3.1(3.5-13.0)	1.6±0.6(0.9-2.5)
Mg^{2+}total	0.2±0.1(0.1-0.5)	0.1±0.1(0.2-0.5)	1.8±0.2(1.5-2.0)	0.7±0.1(0.6-0.8)	0.6±0.5(0.3-1.8)	0.2±0.1(0.1-0.3)
∑WSII**	11.8±4.3(2.8-17.9)	3.9±1.7(1.4-7.2)	10.6±2.9(7.4-14.7)	3.4±1.2(2.2-5.4)	43.8±26.6(25.0-109.5)	15.5±8.1(7.6-34.7)
∑WSII-nss**	11.4±4.3(2.7-17.7)	3.7±1.6(1.2-6.6)	10.2±2.8(7.2-14.3)	3.3±1.2(2.2-5.2)	43.1±26.4(24.3-108.6)	15.3±8.0(7.5-34.4)
%WSII-total***	4.9±2.3(1.0-8.7)	4.7±2.1(1.6-7.3)	3.0±1.0(1.8-4.2)	5.4±1.8(2.7-7.4)	13.2±14.1(2.6-47.2)	12.7±7.2(1.9-22.8)
%WSII-nss***	4.8±2.2(1.0-8.5)	4.4±2.0(1.4-6.8)	2.9±1.0(1.8-4.1)	5.3±1.8(2.6-7.2)	13.0±14.1(2.5-46.8)	12.6±7.1(1.9-22.6)

* represent % contribution of $PM_{2.5}$ and $PM_{2.5-10}$ in $\Sigma PM_{10}(PM_{2.5} + PM_{2.5-10})$ load;**represent sum of total water-soluble inorganic ions and non sea salt ions;

*** percentage contribution of ∑WSII** and ∑WSII-nss to total load of $PM_{2.5}$ and $PM_{2.5-10}$ load; ^ represents minimum and maximum concentrations;

$nss-K^+ = K^+ - (0.037 \times Na^+)$; $nss-Ca^{2+} = Ca^{2+} - (0.0385 \times Na^+)$, $nss-SO_4^{2-} = SO_4^{2-} - (0.253 \times Na^+)$ (Keene et al., 1986; Lu et al., 2018)

Table 2. Correlations between water-soluble inorganic ions in $PM_{2.5}$ and $PM_{2.5-10}$ over Bikaner (BKR), Jhunjhunu (JHJ) and New Delhi (DEL).

BKR									
$PM_{2.5}/PM_{2.5-10}$	F^-	Cl^-	NO_3^-	SO_4^{2-}	Na^+	NH_4^+	K^+	Ca^{2+}	Mg^{2+}
F^-	1	0.47	.66*	.67*	.69*	0.13	.77**	.82**	.64*
Cl^-	0.32	1	0.59	.66*	.87**	0.26	0.26	0.51	0.63
NO_3^-	0.32	1.0**	1	.98**	.76**	.70*	.85**	.78**	.70*
SO_4^{2-}	.77*	0.45	0.45	1	.84**	0.61	.77**	.84**	.77**
Na^+	.68*	0.37	0.37	.96**	1	0.29	0.47	.76*	.81**
NH_4^+	0.28	.71*	.71*	0.16	0.008	1	0.58	0.25	0.21
K^+	0.31	-0.30	-0.30	0.57	0.62	-0.36	1	.74*	0.52
Ca^{2+}	0.5	0.57	0.57	.81**	.72*	0.25	0.28	1	.90**
Mg^{2+}	0.59	0.58	0.58	.88**	.81**	0.27	0.32	.97**	1
JHJ									
$PM_{2.5}/PM_{2.5-10}$	F^-	Cl^-	NO_3^-	SO_4^{2-}	Na^+	NH_4^+	K^+	Ca^{2+}	Mg^{2+}
F^-	1	-0.49	0.32	0.20	-0.24	0.46	0.36	0.66	0.34
Cl^-	0.21	1	-0.29	0.01	0.70	-0.5	-0.30	-0.22	-0.18
NO_3^-	0.65	0.32	1	0.85	0.34	0.30	.99**	0.51	0.59
SO_4^{2-}	0.68	0.66	.90*	1	0.70	0.51	.89*	0.73	0.86
Na^+	0.20	.94*	0.53	0.76	1	0.08	0.38	0.38	0.52
NH_4^+	0.84	0.12	.93*	0.80	0.28	1	0.41	0.84	0.86
K^+	0.78	0.15	.96**	0.83	0.33	.99**	1	0.61	0.68
Ca^{2+}	0.04	0.03	0.75	0.54	0.30	0.55	0.65	1	.91*
Mg^{2+}	0.06	0.50	0.74	0.70	0.76	0.47	0.56	0.79	1
DEL									
$PM_{2.5}/PM_{2.5-10}$	F^-	Cl^-	NO_3^-	SO_4^{2-}	Na^+	NH_4^+	K^+	Ca^{2+}	Mg^{2+}
F^-	1	-0.11	.84**	.83**	.88**	.89**	0.60	0.39	0.36
Cl^-	-0.10	1	0.10	0.18	-0.04	-0.30	0.37	0.43	0.34
NO_3^-	0.50	0.30	1	.96**	.94**	.72*	.88**	.74*	0.65
SO_4^{2-}	0.56	0.37	0.65	1	.92**	.69*	.87**	.74*	.70*
Na^+	0.62	0.09	0.25	.72*	1	.81**	.75*	0.59	0.54
NH_4^+	0.41	0.002	0.40	.69*	0.43	1	0.34	0.11	0.11
K^+	.73*	0.004	.78*	.71*	0.45	0.51	1	.94**	.89**
Ca^{2+}	.70*	-0.08	.77*	0.52	0.51	0.14	.79*	1	.90**
Mg^{2+}	0.61	0.32	0.58	.74*	0.62	0.13	.76*	.72*	1

* Correlation is significant at the 0.05 level;** Correlation is significant at the 0.01 level (2-tailed)

.

Table 3. Concentrations of organic carbon (OC) and elemental carbon (EC) in μgm^{-3} units and other parameters in $PM_{2.5}$ over Bikaner (BKR), Jhunjhunu (JHJ) and New Delhi (DEL).

	BKR	JHJ	DEL
	$PM_{2.5}$	$PM_{2.5}$	$PM_{2.5}$
OC	11.3	7.6	28.2
EC	1.6	1.4	8
TC	12.9	9	36.5
OC/EC	7.1	5.4	3.5
char- EC/soot- EC	1.3	2.2	6.4
TC/EC	8.1	6.4	4.5
K^+/EC	0.4	0.4	0.3
K^+/OC	0.1	0.1	0.1
POC[a]	6.3(57.7 *)	5.1(65.0*)	7.4(30.6*)
SOC[b]	4.9(42.4*)	2.5(35.0*)	20.8(69.4*)
TCM[e]	25.5	17.5	54.3
OM[c]	23.7	15.9	45.1
EM[d]	1.8	1.6	9.1
%TCM	9.4	4.6	13.3
char-EC[f]	0.9	1	6.9
soot-EC[g]	0.7	0.5	1.1
ECR[h]	0.6	0.4	1.3

a.$(OC)_{pri}$=(OC / EC)$_{min}$ × (EC); b. $(OC)_{sec}$=$(OC)_{tot}$ − $(OC)_{pri}$; c.Organic matter (OM) = 1.6 × OC; d. Elemental matter (EM) = 1.1 × EC; e. Total Carbonaceous materials (TCM) = OM + EM; f. Char EC= EC1-OP; g. Soot EC = EC2+EC3; h. Effective Carbon ratio (ECR) = SOC/ (POC + EC) and * indicates the % Contributions of POC and SOC to organic carbon (OC) in brackets.

Table 4. Results of principal component analysis (PCA) of carbon fraction (OC1-OC4, EC1 to EC3 and OP) in $PM_{2.5}$ over Bikaner (BKR), Jhunjhunu (JHJ) and New Delhi (DEL).

Sites	PC1 (%)	PC2 (%)	PC3 (%)	Cumulative (%)
Bikaner (BKR)	76.69	-	-	76.69
Jhunjhunu (JHJ)	74.9	23.4		98.3
New Delhi (DEL)	36.35	33.06	23.82	93.23

Figures

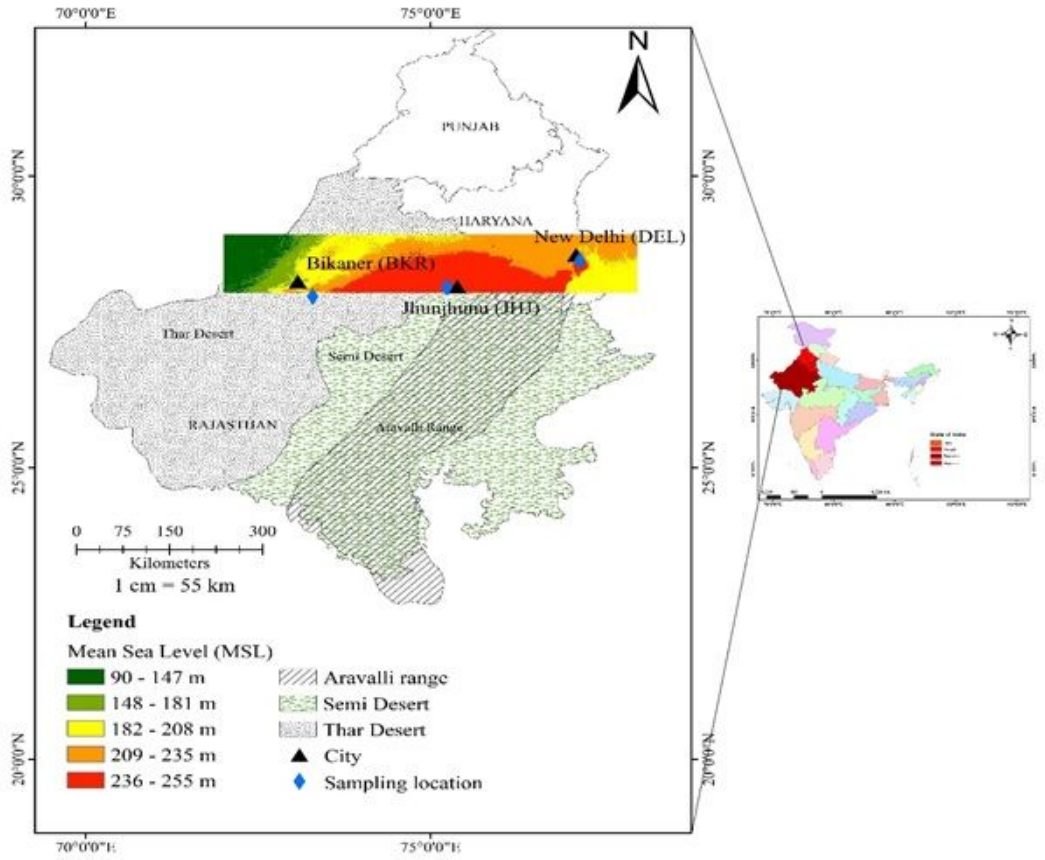

Figure 1

Map showing study area features with particle sampling points and mean sea level (MSL) at Bikaner (BKR), Jhunjhunu (JHJ) and New Delhi (DEL) in the north-north west India. Note: The designations employed and the presentation of the material on this map do not imply the expression of any opinion whatsoever on the part of Research Square concerning the legal status of any country, territory, city or area or of its authorities, or concerning the delimitation of its frontiers or boundaries. This map has been provided by the authors.

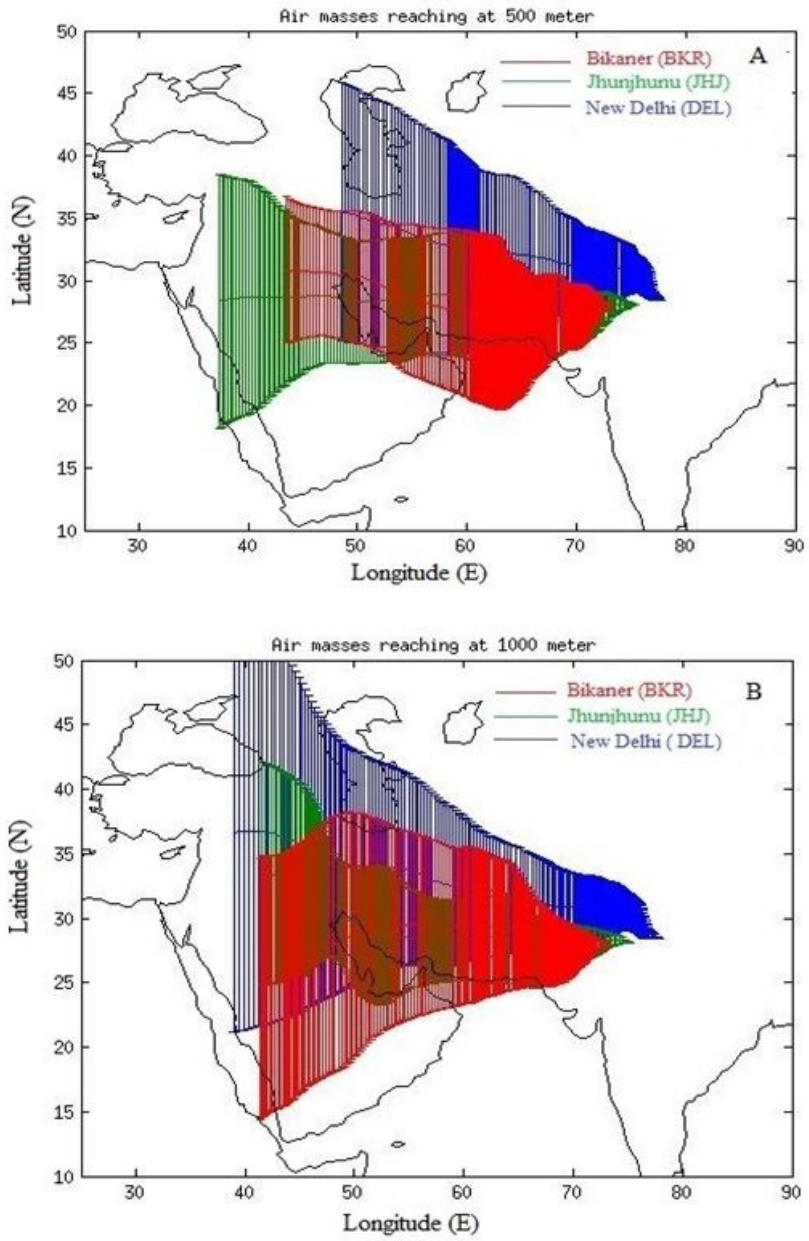

Figure 2

Cluster mean trajectories at 500m and 1000m level over Bikaner (BKR), Jhunjhunu (JHJ) and New Delhi (DEL) during May month-2012 summer seasons Source: National Oceanic Atmospheric Administration (NOAA; http://www.arl.noaa.gov/HYSPLIT.php) (Stein et al., 2015). Note: The designations employed and the presentation of the material on this map do not imply the expression of any opinion whatsoever on the part of Research Square concerning the legal status of any country, territory, city or area or of its authorities, or concerning the delimitation of its frontiers or boundaries. This map has been provided by the authors.

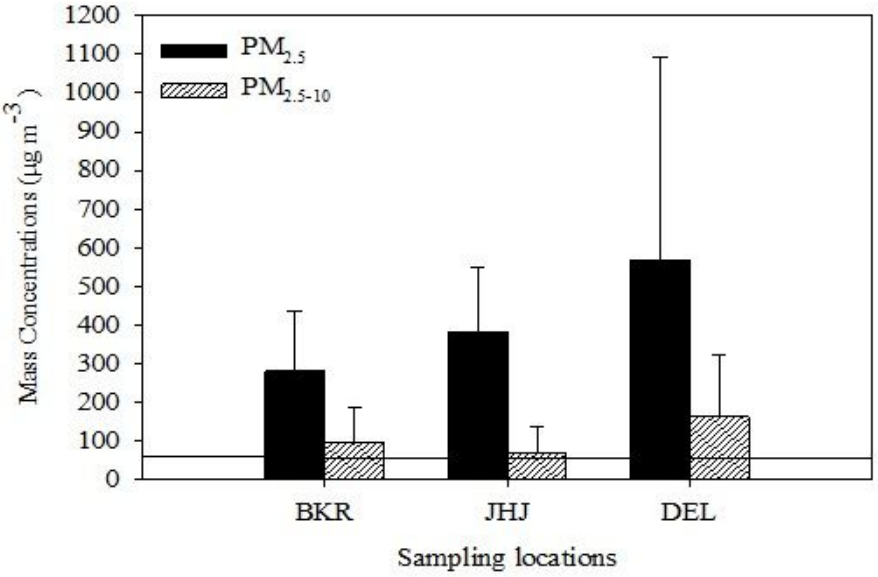

Figure 3

Average mass concentrations of PM2.5 and PM2.5-10 at Bikaner (BKR), Jhunjhunu (JHJ) and New Delhi (DEL) during summer season. Horizontal line represents National Ambient Air Quality Standard limit of 60 µg m-3 for PM2.5 (NAAQS 24 hour's average value).

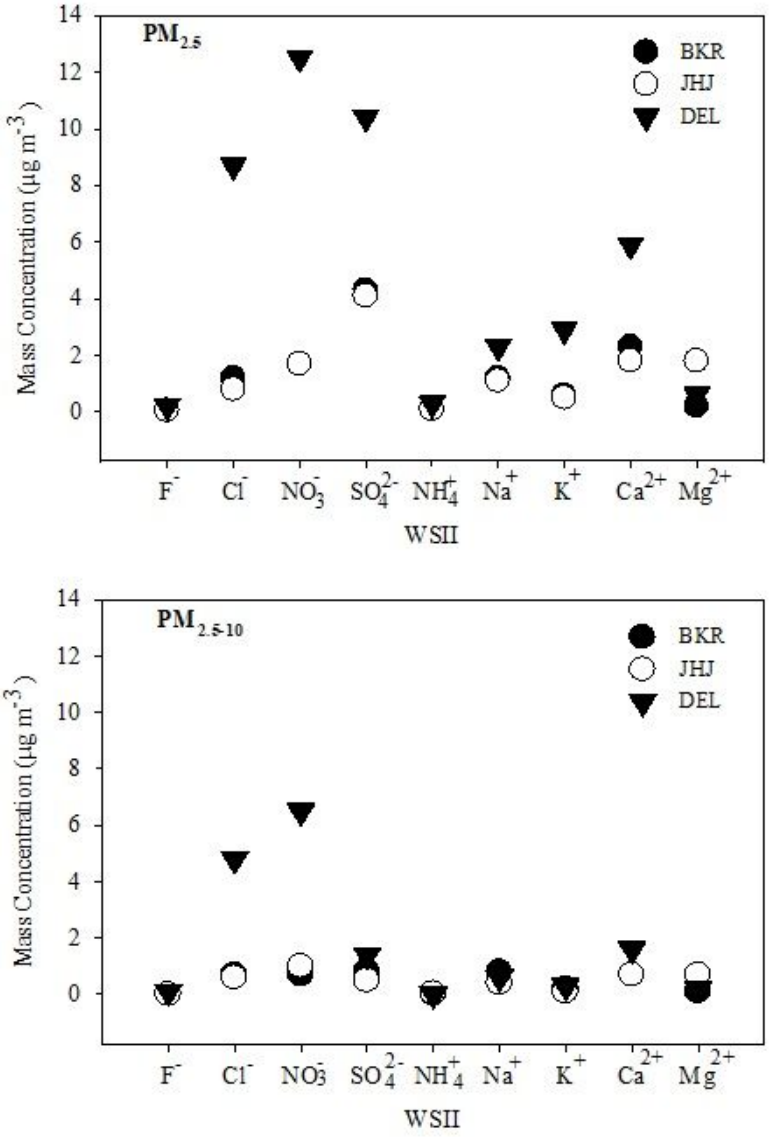

Figure 4

Average concentrations (in µgm-3 units) of water-soluble inorganicions in PM2.5and PM2.5-10 at Bikaner (BKR), Jhunjhunu (JHJ) and New Delhi (DEL).

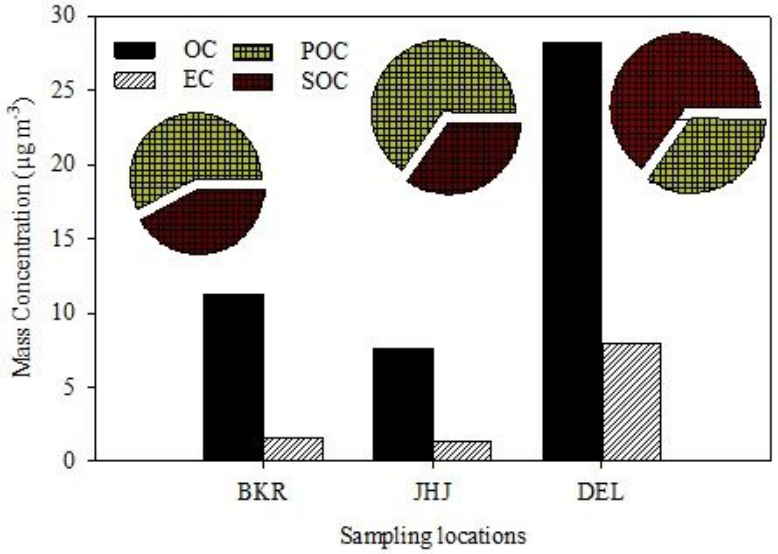

Figure 5

Bar graph and Pie chart showing variations of organic (OC) and elemental (EC) and contributions of primary organic carbon (POC) and secondary organic carbon (SOC) to OC in PM2.5 over Bikaner (BKR), Jhunjhunu (JHJ) and New Delhi DEL).

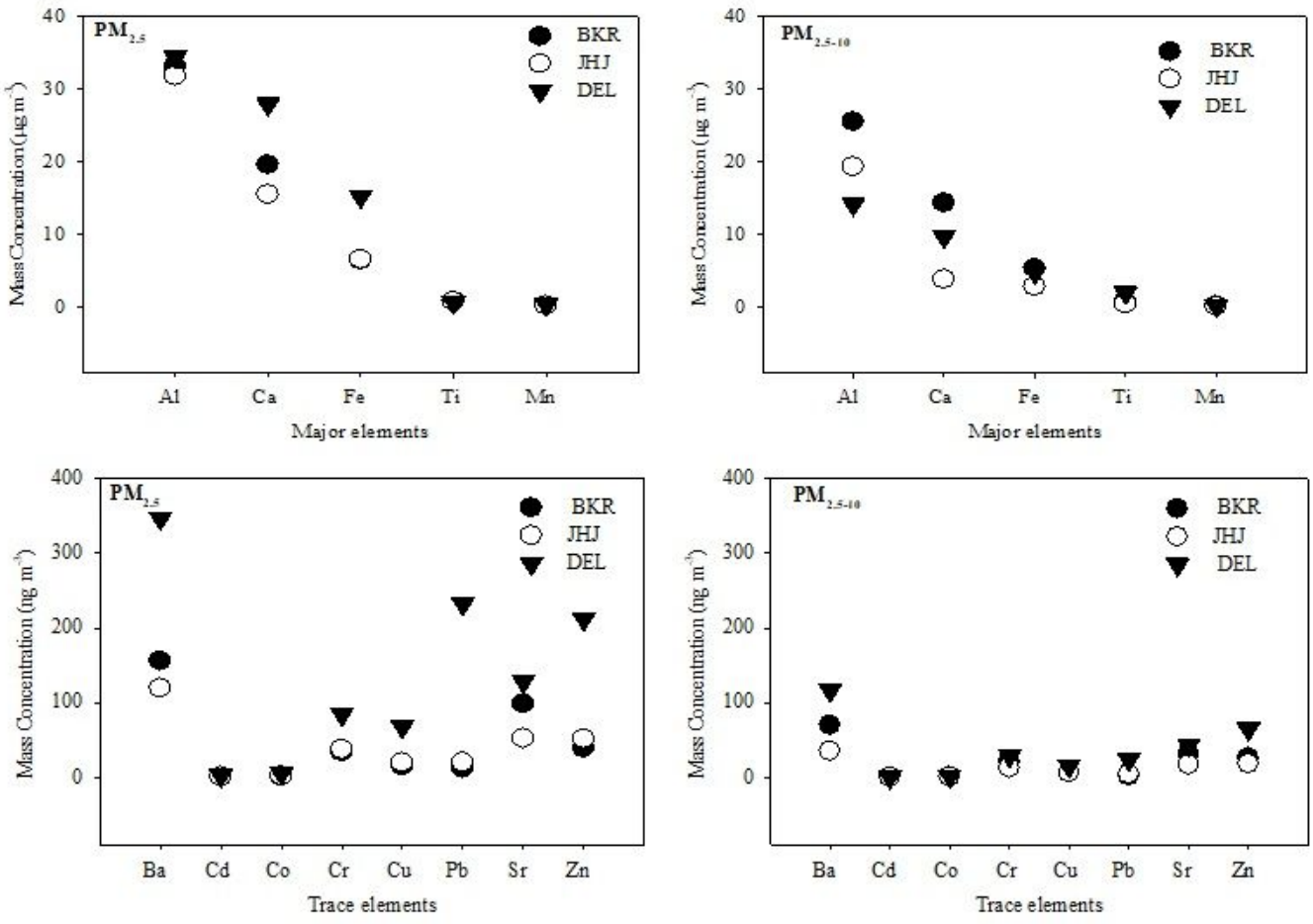

Figure 6

Major and trace element concentrations in water-soluble residue of PM2.5 and PM2.5-10 over Bikaner (BKR), Jhunjhunu (JHJ) and New Delhi (DEL).

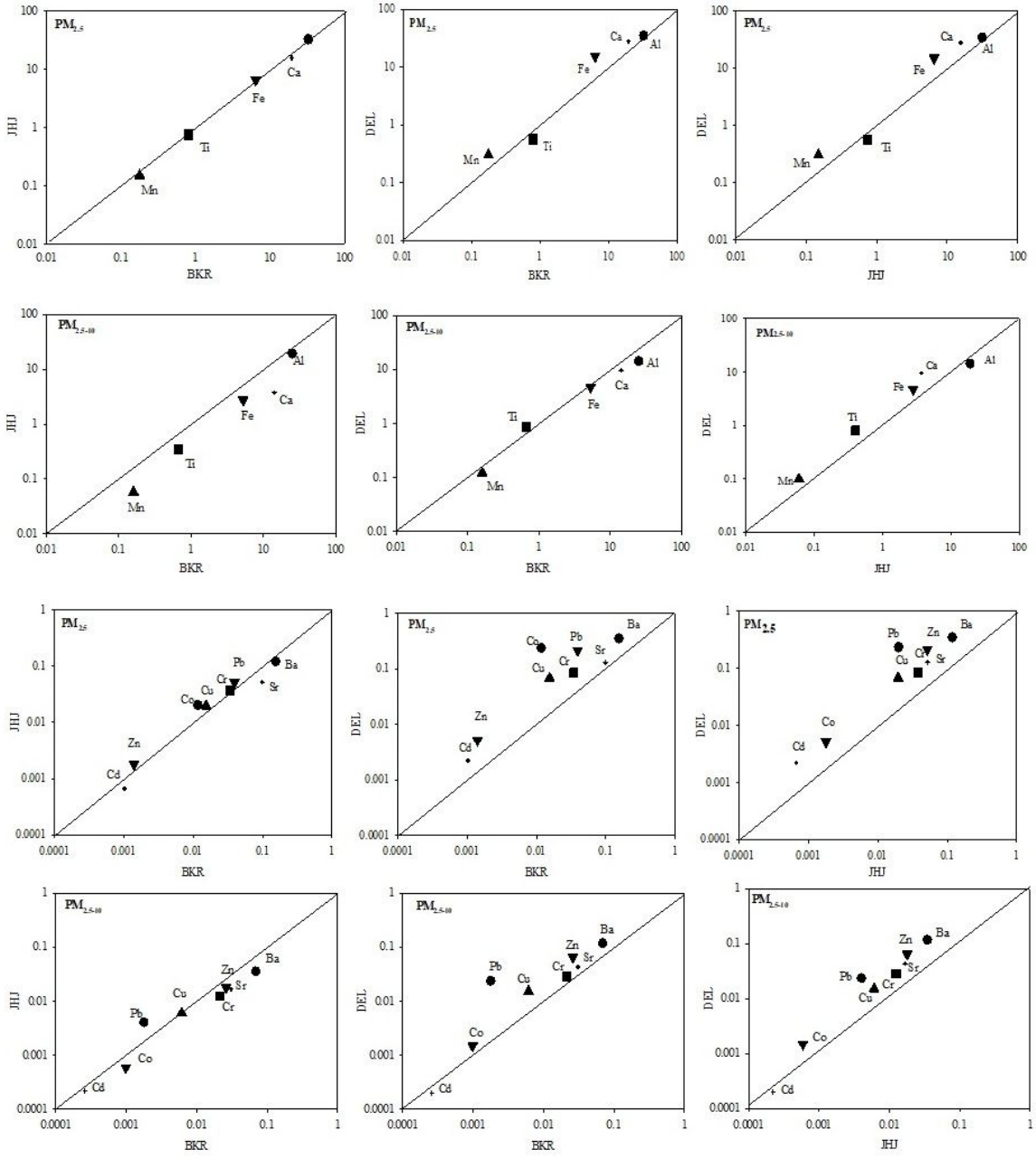

Figure 7

Equiline plot of PM2.5 and PM2.5-10for Major (Al, Ca, Fe, Ti, Mn) and Trace elements (Ba,Sr,Zn,Cr,Pb,Cu,Co,Cd) between Bikaner (BKR), Jhunjhunu (JHJ) and New Delhi (DEL).

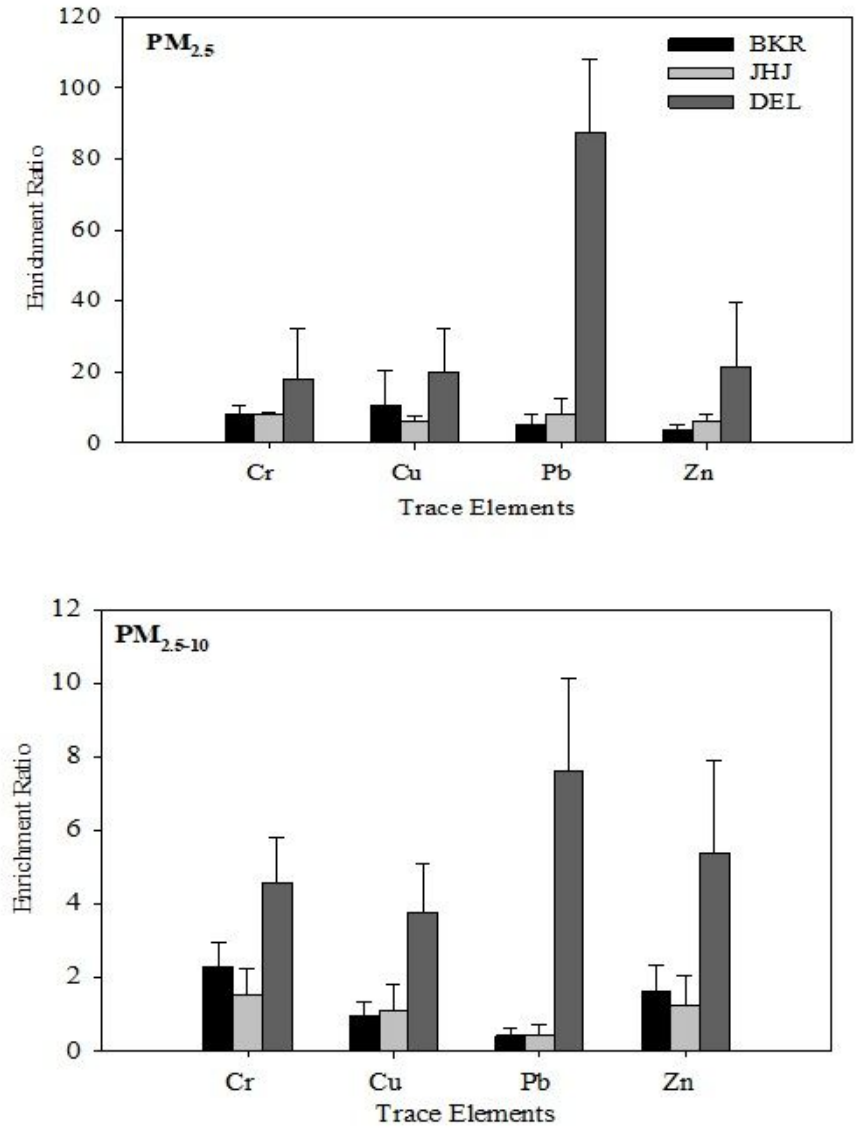

Figure 8

Enrichment ratio (ER) of elements in PM2.5 and PM2.5-10 collected over Bikaner(BKR), Jhunjhunu (JHJ) and New Delhi (DEL) ; ER= (CXs/Als) / (CXC/AlC), where CXs and CXC are the concentration of element X in the sample and upper continental crust (UCC), respectively. Similarly, Als and Alc represent the concentration of Al in the sample and UCC, respectively (UCC values are taken form McLennan , 2001).

Supplementary Files

This is a list of supplementary files associated with this preprint. Click to download.

- SupplimentaryMaterialESM1.docx